Telechelic Associative Polymers: Interactions between Strongly Stretched Planar Adsorbed Layers

Xiao-Xia Meng and William B. Russel*

Department of Chemical Engineering, Princeton University, Princeton, New Jersey 08544

Received June 30, 2003; Revised Manuscript Received October 20, 2003

ABSTRACT: The interactions between planar brushes of adsorbed telechelic polymers are investigated via a self-consistent mean-field calculation via the strong stretching approximation. By allowing the relaxation of the loops upon the initiation of bridging, we obtain a stronger attraction than from Milner and Witten's analysis that excludes this effect. The entropy of ends is the origin of the attraction, but excluded-volume interactions play a role. The interaction potential in kT per chain is determined by the dimensionless separation and a single dimensionless parameter, the extent of stretching normalized by the size of a Gaussian coil.

Introduction

Interactions between surfaces coated with adsorbed polymers control the phase behavior and rheology of a variety of systems, ranging from polymerically stabilized colloids[1] and microemulsions[2−4] to telechelic polymer solutions.[5−10] Fundamental understanding is based on analyses of simple geometries such as planar, cylindrical, and spherical surfaces interacting with homopolymers,[11,12] diblock,[13,14] and telechelic polymers.[15]

Because of the geometrical complexity of interactions between spheres and the typically small ratio of the polymer's size relative to the particle radius, most of the interesting and illuminating work addresses planar brushes. The pioneering analysis of Milner, Witten, and Cates[13] focused on isolated and interacting brushes composed of terminally anchored polymers in a marginal solvent in the strongly stretched limit. Via self-consistent-field theory, they proved that the segments form a parabolic profile, while the chain ends distribute nonuniformly with a bias toward the outer edge of the layer. This profile should be preserved in the highly stretched limit for isolated layers of telechelic chains, since the half chains resemble the full chains of a terminally anchored polymer. However, telechelics can exchange end blocks between two interacting surfaces to gain entropy and decrease the free energy. Hence, an attraction arises from the entropy gain, plus any benefit from a change in the segment distributions, due to the formation of bridges between two surfaces. Milner and Witten assumed that bridges only slightly perturb the loops, so that half chains from bridges and loops would be indistinguishable.[15] That allowed them to predict the relative amounts of bridges and loops with the same partition function from the self-consistent-field calculation. This resulted in a weak attraction (less than $0.1kT$ per chain) at "classical contact", when the separation between the two plates is twice the thickness of an isolated brush. They attributed the attraction to thermal fluctuations of loops with midpoints near the edge of the layer, allowing the end (midpoint) distributions to overlap. This assumption seems to preclude the possibility of loops relaxing and bridges assuming more extended configurations in order to lower the free energy.

Johner and Joanny[16] applied the asymptotic strong stretching theory to chains grafted to one plate with a free end that tends to adsorb to a second plate, allowing for both bridges and free ends. No loops exist, and the fraction of bridges approaches unity when the energy of adsorption is high. Bjorling[17] adopted the analysis of Joanny and Johner to examine the interaction between plates coated by telechelic polymers, by allowing the polymers to form either bridges or loops between two interacting plates. The interaction proved to be attractive for a brush interacting with a bare surface, i.e., the asymmetric case, but repulsive for the symmetric case in which both plates have the same coverage. The absence of attraction was ascribed to the absence of thermal fluctuations, but, in fact, the entropy gain due to end exchange was neglected.

While several groups have analyzed the structure of cylindrical and spherical brushes, predicting the interaction potential is nontrivial. Ball et al.[18] formulated the asymptotic approximation for cylindrical and spherical brushes composed of strongly stretched diblocks, i.e., polymers having only one adsorbing block each. They constructed an analytical solution for the cylindrical brush but not for the spherical brush. Clearly an exact analytical treatment of interactions between two spheres is completely out of the question. Li and Witten estimated the free energy of a spherical brush from a variational approach but did not address interactions.[19] Lin and Gast solved the self-consistent-field equations numerically for a spherical brush and constructed the interaction potential between two interacting brushes of diblocks, i.e., without bridging, from the cost of isotropic compression.[20] Not surprisingly, they found a repulsive interaction. This simple but important case is the basis for polymeric stabilization of colloidal dispersions but does not address telechelic layers.

A more generally tractable approach to the spherical case is to start with the planar brush and then approximate the spherical geometry via a perturbation expansion. From the analysis of planar brushes by Milner and Witten, Semenov et al.[21] constructed a scaling analysis to describe the interaction between telechelic micelles, the transition between dilute and

* Corresponding author: e-mail wbrussel@princeton.edu.

10.1021/ma0349027 CCC: $25.00
Published on Web 12/03/2003

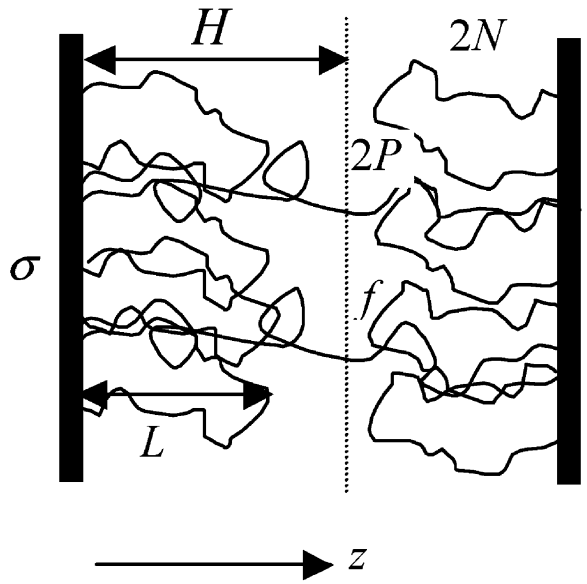

Figure 1. Schematic of the planar geometry with a fraction f of the chains with $2N$ segments each forming bridges with $2P$ segments residing between layers of loops with thickness L. The surfaces with σ chains adsorbed per area are $2H$ apart.

condensed phases, and the modulus for close-packed micellar phases. Subsequently, Pham et al.[22] observed that associative polymers in aqueous solutions phase separate into gas and liquid phases at concentrations of less than a few percent, which confirms the attraction anticipated by Semenov and co-workers. With Semenov's interaction potential and a molecular theory they constructed a correlation for the observed gas−liquid phase transition and high-frequency moduli for percolated phases.[6,22]

Here we seek a more quantitative description of the interactions between planar surfaces bearing adsorbed telechelic polymers. We formulate the free energy of interacting planar brushes consisting of parabolic layers separated by a homogeneous region of bridges and then minimize to obtain the equilibrium potential per half chain Φ, along with the fraction of bridging chains f, number of bridging segments P lying beyond the loops, and thickness L of the layer of loops. Although not included explicitly, thermal fluctuations are implicit in the ability of bridging chains to extend beyond the loops to allow end-block/stickers to exchange from one surface to the other. The result is a fairly strong attraction (still less than $0.69kT$ per chain, which is the attraction between Guassian brushes) between telechelic brushes, facilitated by the ability of layers of loops to shrink when bridges form, as Bjorling reported.

Theory

Figure 1 depicts telechelic polymers with $2N$ segments adsorbed on two planar surfaces at a density of σ chains per unit area on each surface. We assume all the ends to reside on the surfaces, forming either loops or bridges. At equilibrium, loops reach a maximum distance L from the surface, whereas a fraction f of the chains form bridges between surfaces $2H$ apart. When L is less than H, $2P$ segments of a bridge will reside in the gap between loops. When the two plates are far apart, chains can only form loops that produce a layer of thickness L_∞, which is our base state.

In a dense brush composed of loops, chains are highly stretched, allowing us to assume that midpoints connect two-half chains with trajectories that lead monotonically toward a surface, though not necessarily the same one. Hence, we can cut the loops at the midpoint into halves without changing the configurations. Inside the layer, the chains are stretched nonuniformly by a potential that varies with position to allow chains that start at any point to reach a surface in N segments. Milner, Witten, and Cates[13] employed the analogy to the movement of a harmonic oscillator to prove that the potential must be parabolic to satisfy the constraint. The oscillator starts at an arbitrary position and is accelerated from rest by a parabolic potential to return to the equilibrium position in one-quarter of the period. The chains in a brush are analogous to oscillators with the number of segments and stretching in the chains corresponding to time and velocity. The midpoints of loops are free of tension, so the chains must be accelerated to the surface from zero initial velocity.

We can also treat the chains of bridges as two subchains connected at the midpoint, but the midpoint bears a finite tension due to the excess stretching required to reach both surfaces. This distinguishes a bridge from a loop. The tension on the ends of half bridges keeps the half chains from relaxing into the layers. Segments that reside in the gap between layers feel a uniform potential, while the segments within the layer are accelerated by the parabolic potential. Hence, the bridges enter the layer with a nonzero initial velocity and are accelerated to the surface in fewer, i.e. $N-P$, segments.

We start by identifying contributions to the free energy for strongly stretched chains. Constraints that govern the free energy are then discussed. In the infinite separation limit, we recover the same base state as Bjorling and Johner and Joanny.

Free Energy. There are three components in the free energy: configurational entropy due to stretching of the chains, excluded volume due to the fact that segments must avoid each other, and the entropy of the ends. Hence, the free energy per half chain is the sum of the three

$$A = A_{st} + A_{ex} + A_{en} \tag{1}$$

and the interaction potential per half chain Φ referred to the isolated brush with free energy A_∞ is

$$\Phi = A - A_\infty \tag{2}$$

We take the unit of energy to be kT in all cases and average over all chains to obtain the free energy per half chain.

The energy due to stretching A_{st} is analogous to the kinetic energy of a harmonic oscillator with the Hamiltonian $(dz/dn)^2/2$, where z is the coordinate normal to the surface that prescribes the location of the nth segment of a chain. Since the midpoints of the chains (or the ends of the half chains) have a distribution of $\epsilon(z_0)$ chains per volume, the average free energy per half chain is

$$A_{st} = \frac{1}{4\sigma}\int_0^H \epsilon(z_0)\int_0^N \left(\frac{dz}{dn}\right)^2 dn\, dz_0 \tag{3}$$

Here we follow the convention that the mean-square

end-to-end distance is $3Nl^2$ for a half chain and set the length of a segment l to be the unit of length.[16,23] The factor $1/(2\sigma)$ accounts for 2σ half chains per unit area on each plane, which requires the end distribution to satisfy $\int_0^H \epsilon(z_0)\, dz_0 = 2\sigma$. The end distribution and dz/dn both depend on whether the chain forms a bridge or a loop, as we discuss in the next section.

The excluded volume in the mean-field approximation is proportional to the square of the segment density, ϕ^2, with a proportionality constant determined by the segmental excluded volume v. For a half chain

$$A_{ex} = \frac{v}{4\sigma}\int_0^H \phi^2(z)\, dz \tag{4}$$

where $\phi(z)$ has contributions from the loops and bridges in the layer

$$\phi(z) = \phi_b(z) + \phi_l(z) \tag{5}$$

but only bridges contribute in the gap.

The entropy of ends can be calculated by counting the configurations. In a unit area, the number of configurations Ω available to the 2σ chains in the gap is

$$\Omega = \frac{(2\sigma)!}{(2\sigma f)![2\sigma(1-f)]!} \tag{6}$$

Note that the distinguishable configurations are loops or bridges, independent of which surface they reside on. Hence, the entropy per half chain follows as

$$A_{en} = -\frac{1}{4\sigma}\ln \Omega \tag{7}$$

When the number of chains is large, which is true in a dense brush, Stirling's approximation holds for a dummy variable x

$$\ln x! = x \ln x - x \tag{8}$$

so that the free energy per half chain due to ends is

$$A_{en} = \frac{1}{2}[f \ln f + (1-f)\ln(1-f)] \tag{9}$$

This is analogous to the entropy of mixing for binary mixtures. Since both ends are reversibly adsorbed onto the surfaces, either or both can move from one surface to the other. Dai et al. observed this when bringing telechelic polymers adsorbed on a surface into contact with bare mica in a surface force apparatus.[24] The same result would follow from starting with half chains and realizing that two halves from a chain must connect to each other.

To evaluate each contribution, we need to know the end distribution $\epsilon(z_0)$, segment density $\phi(z)$, and local stretching dz/dn. Then by minimizing the free energy, the equilibrium configurations and the interaction potential can be determined.

Constraints. We need to minimize the free energy with respect to the parameters that define the configurations, i.e., the thickness of the brush L, the number of bridging segments in the gap P, and the fraction of bridges f. However, constraints are imposed among these parameters by the conservation of mass, the tension at the midpoints of loops and bridges, and the requirement of equal number of segments to reach the surfaces from the midpoint for both loops and bridges. We focus on these constraints in this section.

Since the potential $U(z)$ must be parabolic for all chains to reach the surface in an equal number of segments (by analogy to a harmonic oscillator)[13]

$$U(z) = -(B_1 - B_2 z^2) \tag{10}$$

with B_1 and B_2 constant. In a marginal solvent, the potential is proportional to the segment density $\phi(z)$[15]

$$U(z) = -v\phi(z) \tag{11}$$

so $\phi(z)$ also must be parabolic.

Within the parabolic profile, the equation of motion for the nth segment on a half chain is

$$\frac{d^2z}{dn^2} = -\frac{dU}{dz} = -2B_2 z \tag{12}$$

with boundary conditions that $n = 0$ where $z = 0$, $dz/dn = 0$ where $n = N$ and $z = z_0$ for loops with z_0 being the midpoint of a loop, and $n = N - P$ where $z = L$ for bridges. The solution of the equation relates the position z to the segment number n as

$$z = C_1 \sin\sqrt{2B_2}\, n \tag{13}$$

and the tension follows as

$$\frac{dz}{dn} = C_1\sqrt{2B_2}\cos\sqrt{2B_2}\, n \tag{14}$$

Hence, from the boundary conditions $B_2 = \pi^2/8N^2$ and $C_1 = z_0$ for loops and $C_1 = L/\cos(\pi P/(2N))$ for bridges. At the edge of the layer, the tension of the bridge is continuous with that in the gap, which is $(H - L)/P$. Applying this boundary condition to eq 14 leads to

$$\frac{H-L}{L} = \frac{P\pi}{2N}\tan\left(\frac{\pi P}{2N}\right) \tag{15}$$

which is consistent with eq 4.3 in Johner and Joanny's paper.

The segment density at position z has contributions from all chains that start from a distance $z_0 > z$ and reach z with stretching dz/dn:

$$\phi(z) = \int_z^H dz_0\, \epsilon(z_0)\left|\frac{dz}{dn}(z_0, z)\right|^{-1} \tag{16}$$

where $\epsilon(z_0)$ is the end density. For bridges, all midpoints reside at H, so $\epsilon(z_0) = 2\sigma f\,\delta(H - z_0)$ and the integral reduces to the segment density from bridges ϕ_b

$$\phi_b(z) = \frac{2\sigma f P}{H - L} \tag{17}$$

in the gap. Thus, $U(L)$ is determined by eqs 10, 11, and 17, which implies

$$B_1 = B_2 L^2 + \frac{2\sigma f P v}{H - L} \tag{18}$$

The total number of segments in the parabolic region

$$-\int_0^L \frac{U(z)}{v}\, dz = 2\sigma[(1-f)N + f(N-P)] \tag{19}$$

then determines the relation between L, P, and f from eqs 10, 18, and 19 as

$$f = \frac{N}{P}\left(1 - \frac{L^3}{L_\infty{}^3}\right)\left(1 - \frac{L}{H}\right) \tag{20}$$

where

$$L_\infty = 2\left(\frac{3\sigma v}{\pi^2}\right)^{1/3} N \tag{21}$$

Within the layer, the end distribution is a delta function for bridges and dn/dz follows from eqs 13 and 15

$$\frac{\mathrm{d}n}{\mathrm{d}z} = \left[\frac{\pi^2}{4N^2}(z_0{}^2 - z^2) + \left(\frac{H-L}{P}\right)^2\right]^{-1/2} \tag{22}$$

so that eq 16 determines the contribution from bridges

$$\phi_{\mathrm{bl}}(z) = 2\sigma f\left(\frac{\pi^2}{4N^2}(L^2 - z^2) + \left(\frac{H-L}{P}\right)^2\right)^{-1/2} \tag{23}$$

for $0 < z < L$. Inverting eq 16 with the total number of segments constant, Johner and Joanny obtained the end distribution of loops[16]

$$\epsilon(z_0) = \frac{\pi^2}{4N^3 v} z_0 (L^2 - z_0{}^2)^{1/2} \times \left[1 + \frac{2\sigma f v}{\frac{H-L}{P}\left(\frac{\pi^2}{4N^2}(L^2 - z_0{}^2) + \left(\frac{H-L}{P}\right)^2\right)}\right] \tag{24}$$

The constraints from eqs 15 and 20 leave only one free variable at a fixed separation H. Scaling the lengths L and H by L_∞, P by N, and minimizing the free energy with respect to P/N by setting

$$\frac{\mathrm{d}A}{\mathrm{d}(P/N)} = 0 \tag{25}$$

allows us to calculate L/L_∞, P/N, and f as functions of H/L_∞ and a single parameter $(\sigma N^{3/2} v)^{1/3}$, which is proportional to $L_\infty/N^{1/2}$ from eq 21.

We can compare the free energy with that of an isolated plate by setting $H \to \infty$ and $f = 0$, so that $L = L_\infty$ from eq 20, and $P = N$ from eq 15. Our free energy (1) reduces to

$$\frac{A_\infty}{kT} = \frac{3}{10}(3\pi\sigma v N^{3/2})^{2/3} \tag{26}$$

The thickness and the free energy of the brush are consistent with eqs 2 and 4 in Bjorling's paper.[17]

Results

From eqs 15, 20, and 25, we calculate P/N, L/L_∞, and f as a function of H/L_∞ to define the equilibrium configuration of the brushes. We find that the layers relax as two brushes approach and bridges form. Thus, $L < H$ and $P > 0$. Allowing the configurations of bridges to differ from those of loops lowers the free energy below that derived by Milner and Witten. Consequently, we uncover a different scaling of the free energy and the range of interaction by fitting the strength and range

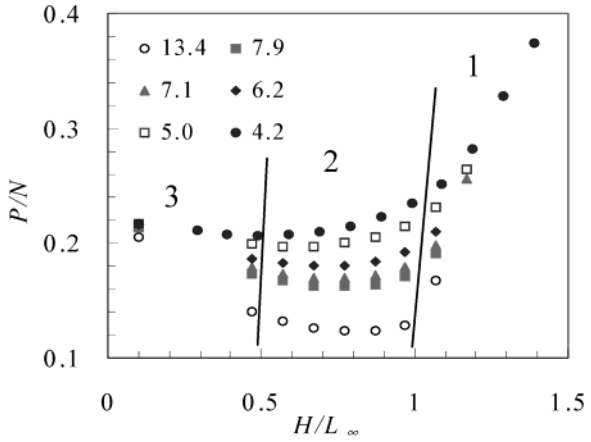

Figure 2. Number of segments in the gap vs separation for different degrees of stretching $L_\infty/N^{1/2}$: stage 1, at or beyond classic contact; stage 2, weak compression with distinct bridges and loops; stage 3, strong compression with indistinguishable loops and bridges.

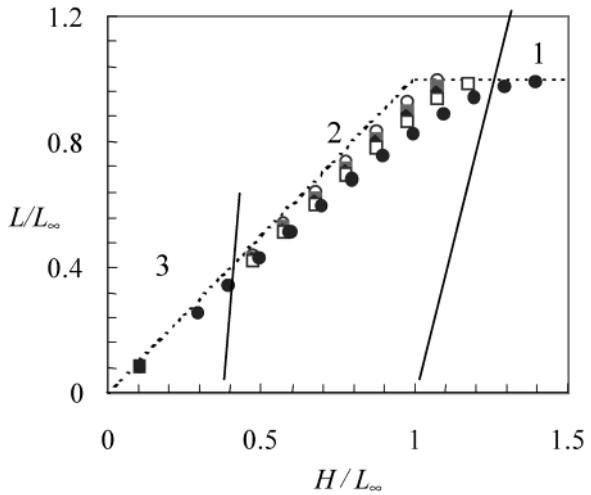

Figure 3. Equilibrium layer height as a function of separation: symbols as in Figure 2; (- - -) prediction of Milner and Witten with $f \ll 1$.

of the attraction to a power law of the degree of stretching. Our statement on relaxation of loops is also visualized by the equilibrium end distribution, which shows all ends residing within $L < L_\infty$, except for those associated with bridges for $H < \infty$.

We can distinguish three stages in terms of the configuration of loops and bridges as two plates approach from infinity, as indicated in Figures 2−4.

Stage 1. For $H > L_\infty$, thermal fluctuations allow the ends of chains originally on one surface to sample the other surface and form bridges. This process only perturbs slightly the equilibrium configuration of the isolated layers as long as $f \ll 1$. The fraction of bridges f increases exponentially with decreasing separation when f is small, as shown in the inset of Figure 4, which is consistent with the prediction of Milner and Witten.[15] A bridge lowers the free energy of the chains due to excluded volume by distributing as many segments as possible in the gap. Although the change in L/L_∞ is very small, the net change in energy due to stretching and excluded volume is still comparable to $f\,kT$ since each contributes many kT's of energy. For instance, the energy due to stretching and the excluded volume increases by $0.00054kT$ when the bridging fraction is 0.00012 with $L_\infty/N^{1/2} = 7.1$.

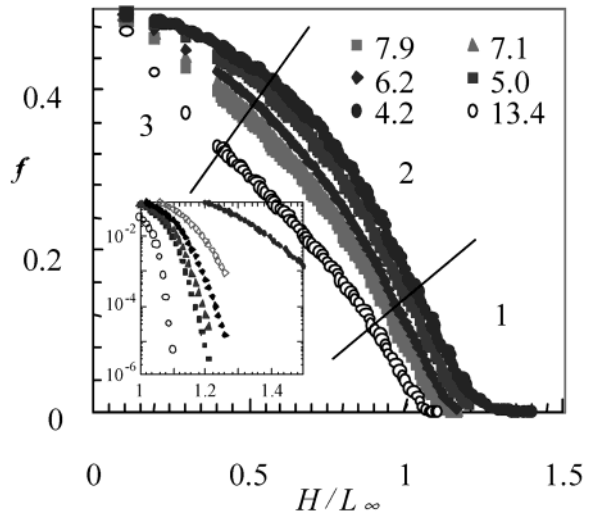

Figure 4. Fraction of the bridges as a function of separation: symbols as in Figure 2; inset showing the exponential decay at large separations.

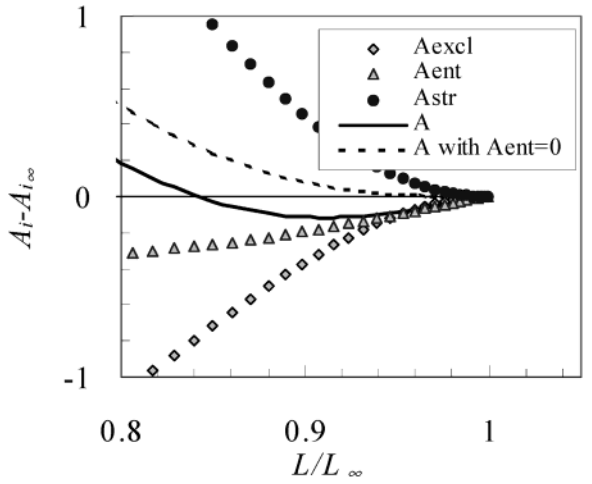

Figure 5. Contributions to the free energy for $H/L_\infty = 1$ and $L_\infty/N^{1/2} = 6.2$.

Stage 2. When the separation roughly equals that at classical contact, i.e., $H \sim L_\infty$, many chains form bridges and the parabolic density profile adjusts to satisfy the requirement that both bridges and loops reach the surface in a fixed number of segments. As a result, the loops relax and allow even more chains to form bridges, which further decreases the excluded-volume contribution to the free energy by distributing segments in the gap. The energy due to stretching increases more quickly as more chains are stretched into the gap, as shown in Figure 5. Hence, the fraction of bridges increases monotonically when brushes are compressed, but not as fast as in stage 1. The energy penalty for stretching also discourages segments from residing in the gap as the concentration builds up due to bridging, which decreases P/N. Hence, bridging allows chains to escape excluded volume in the layer but requires more stretching and builds up excluded-volume interactions in the gap. Nonetheless, we have a much higher fraction of bridges than predicted by Milner and Witten in this regime, especially for high surface densities. The bridging fraction sets the optimum free energy.

Stage 3. When the brushes are compressed to a small separation, segments from bridges start to fill the gap. At this point, the chains pay little penalty by converting from loops to bridges or vice versa and f approaches a half, which maximizes the entropy of the ends. P/N increases slightly for brushes with high surface coverages because of the overcrowding in the layer. The chains feel the potential as if in a melt, where chains become ideal as excluded-volume interactions are screened. The entropy gain due to end exchange decreases the free energy, while the compression of chains increases the free energy. The balance of these two determines the potential.

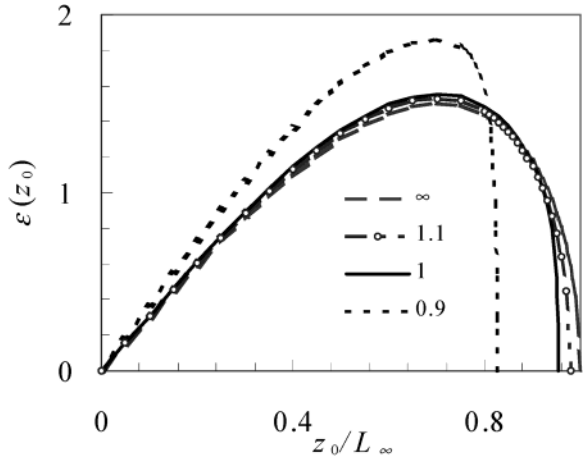

Figure 6. End distribution with the presence of bridges for $L_\infty/N^{1/2} = 6.2$ at separations $H/L_\infty = 0.9 - \infty$.

We plot in Figure 5 each contribution to the free energy for $H/L_\infty = 1$ and $L_\infty/N^{1/2} = 6.2$ as in eqs 3, 4, and 9. The excluded-volume interactions always decrease while the stretching energy and the entropy of ends increase as bridges form. The difference between the contributions from excluded volume and stretching is positive and decreases as the layer thickness increases. The layer thickness at which the total free energy is minimized determines the equilibrium thickness of the brush L, which is somewhat less than the separation H, consistent with our results in Figure 3. The effect of the end exchange on the free energy is pronounced. Without entropy gain due to exchange of ends, as discussed by Bjorling, the free energy always increases with decreasing separations, which indicates repulsion for the full range exactly as Bjorling reported.[17] The end distribution for half chains in the layer plotted in Figure 6 clearly shows the relaxation of loops: the layer thickness is much smaller than the smaller of L_∞ or H. In Milner and Witten's theory, the loops are compressed rather than relaxing voluntarily, which implies that the layer thickness differs from half of the separation by the amount that the thermal energy allows. The area under each curve, $2\sigma(1 - f)$, indicates the number of bridges.

The free energy per chain corresponding to each configuration from eq 1 shown in Figure 7 indicates an attraction that increases with decreasing surface coverage but never exceeds the $0.69kT$ per chain obtained from ideal chains.[25] The width of the attractive well also decreases with increasing density of the brush, indicating the stiffness of the brushes. The softer brushes relax more easily, which allows more chains to form bridges.

Since bridges need *not* be described by the same partition function as loops, as required by Milner and Witten, the free energy should be lower. As shown in Figure 8, the self-consistent-field calculations of Milner

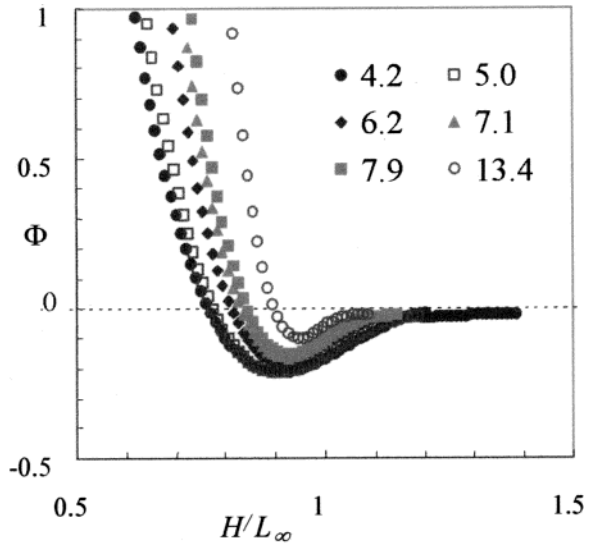

Figure 7. Interaction potential as a function of separation: symbols as in Figure 2.

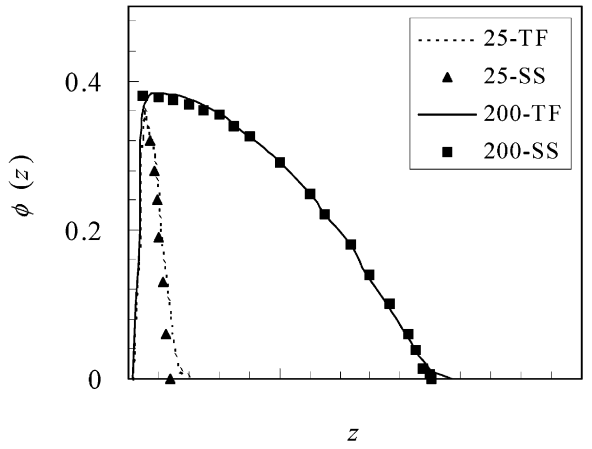

Figure 8. Segment distribution with and without thermal fluctuations for $N = 25$ and 200: TF stands for thermal fluctuations while SS is strongly stretched (replotted from ref 21).

and Witten show that thermal fluctuations increase the layer thickness, indicated by a nonzero segment distribution beyond the strongly stretched layer thickness. However, the fraction of segments reaching beyond the strongly stretched layer thickness was always very small, accounting for the weak attraction. Comparing the largest distance a chain can extend with and without thermal fluctuations allows us to quantify the contribution to the layer thickness from thermal fluctuations to show, as did Milner, that the effect decreases with increasing stretching.[26] For example, when N increases from 25 to 200 with v and σ fixed, the expansion of the brush by thermal fluctuations decreases from 50% to 7% with respect to the strongly stretched layer thickness. Hence, two less dense brushes overlap due to thermal fluctuations, but relaxation of the brush to form a gap can lower the free energy even further. Relaxation of loops becomes more important as the layer becomes denser and stiffer, so the discrepancies between our theory and Milner and Witten's theory increase with stronger stretching.

From Figure 9, we also see that the attraction correlates well with the number of bridges, arising primarily from the entropy of the ends as the contributions from excluded volume and stretching mostly cancel out. Allowing for a gap reduces excluded-volume interactions for bridges, thus increasing the fraction of bridges and shifting the scaling of the free energy to $N^{1/2}/L_\infty$ rather than $(N^{1/2}/L_\infty)^2$, as found by Milner and Witten. The range of the interaction is defined by the width of the interaction potential W

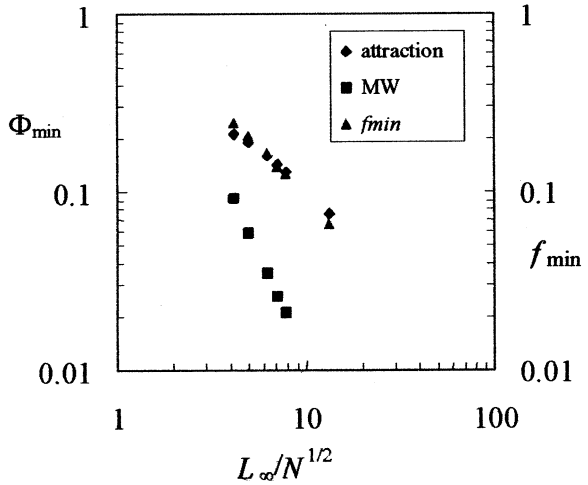

Figure 9. Depth of the attraction and the fraction of bridges compared with Milner and Witten's theory.

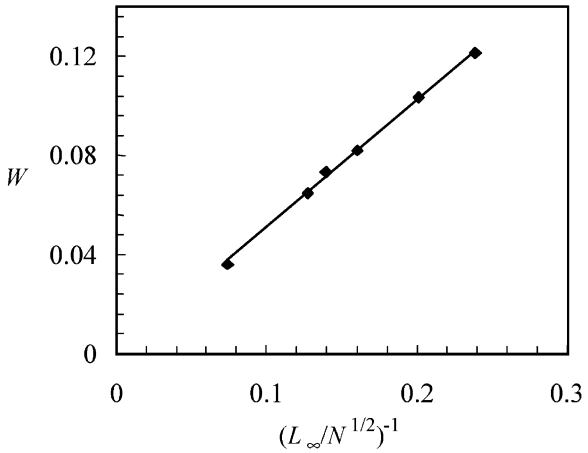

Figure 10. Width of interaction well as a function of stretching fit to $W = 0.51N^{1/2}/L_\infty$.

$$W = \left(\frac{-\Phi}{\mathrm{d}^2\Phi/\mathrm{d}H^2}\right)_{\min}^{1/2} \tag{27}$$

We scale the interaction potential by the depth and the separation by the width with the relations obtained from Figures 9 and 10:

$$\Phi_{\min} \sim (L_\infty/N^{1/2})^{-1} \tag{28}$$

and

$$W \sim (L_\infty/N^{1/2})^{-1} \tag{29}$$

Brushes are "softer" with more bridging chains, as shown in Figure 10. The position of the minimum, which depends on the surface coverage as

$$H_{\min} = 0.232 \arctan(0.735L_\infty/N^{1/2}) + 0.62 \tag{30}$$

as shown in Figure 11, serves as the reference separa-

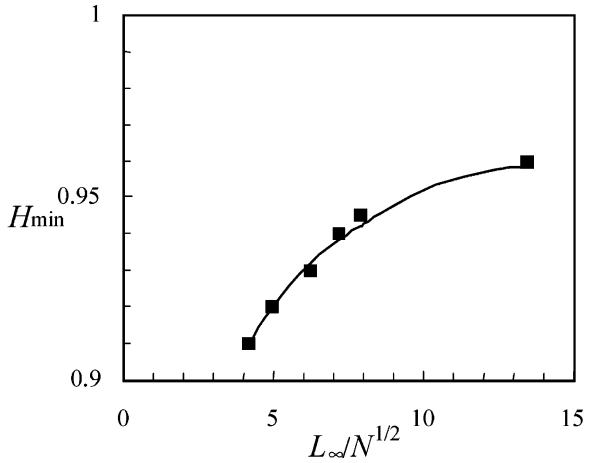

Figure 11. Position of the attractive minimum as a function of stretching. Solid line is fit to eq 30.

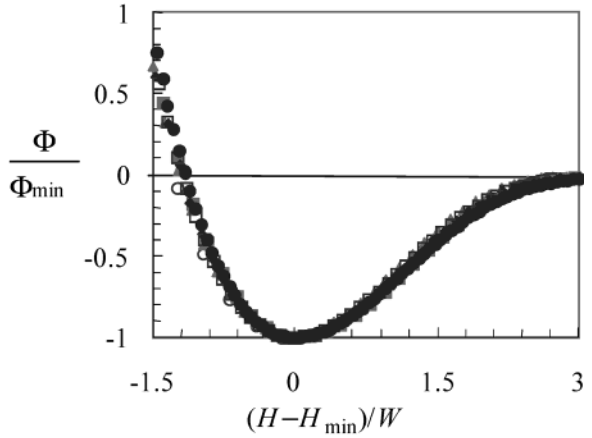

Figure 12. Interaction potential scaled on the minimum and width: symbols as in Figure 2.

tion in our scaling. Equation 30 is not a unique fit but bounds the separation at infinite stretching by unity. The master curve

$$\frac{\Phi}{\Phi_{min}} = f\left(\frac{H - H_{min}}{W}\right) \tag{31}$$

collapses the interaction potentials nicely, as shown in Figure 12. Since $L_\infty/N^{1/2} \propto N^{1/2}$ (eq 21), stronger stretching has the same effect as longer chains when the other parameters such as the grafting density and excluded-volume parameter are fixed.

Conclusions

The free energy per chain has three components in highly stretched brushes of telechelic associative polymers in a marginal solvent: stretching, excluded volume, and entropy due to the exchange of ends. The segment density is parabolic within the layers where loops and bridges coexist and constant in the gap where only bridges exist. Constraints arise to ensure that all half chains end at the surface in the same number of segments for loops, wherever they start, and for bridges that begin on the midplane. We calculated the layer thickness of the loops, the fraction of bridges, and the number of segments from each bridge that reside in the gap at equilibrium. We found that when brushes of loops relax to heights only slightly shorter than at infinite separation, a significant number of segments reside in the gap.

The relaxation of loops has a fairly important effect on the attraction between brushes. Relative to Milner and Witten's theory in which this effect was neglected, the attraction is several times stronger and the fraction of bridges is much higher. The difference increases with surface coverage and, hence, degree of stretching. Likewise, the entropy gain due to the exchange of ends, neglected by Bjorling, provides the driving force for loops to relax and bridges to form. When this effect is neglected, the interaction between brushes predicted by the strong stretching theory becomes purely repulsive, which is not consistent with experimental observations. By considering all the factors, we obtain the lowest free energy among the available theories. A master curve is obtained when we scale the interaction potential and the range of attraction by $N^{1/2}/L_\infty$.

Our theory does not reduce to the ideal case when the chains are Gaussian because the highly stretched assumption does not allow the chains to wander up the potential gradient as can Gaussian chains. Likewise, energy due to compression is missing, which should become important at small separations. Our attraction is bounded above by that of ideal chains ($0.69kT$/chain) when the stretching is small, as it should be according to Bhatia et al.[25]

Our approach presumes the chains to be highly stretched, which might not be true in experiments. However, the correction to the entropy due to the ends should ensure physically reasonable results even for low grafting densities. Indeed, Matsen[23] relaxed the constraint preventing ends of chains from extending beyond the midplane or layer thickness L, producing an end distribution with an exponentially decaying tail that allows the brushes to interpenetrate. This had notable effects on the segment density profile and the free energy, especially for weakly stretched chains. The mean-field calculation of Netz and Schick[27] in the continuum limit for end-anchored chains noted a deviation of the segment density profile from parabolic with weakly stretched chains. They also found that tension exists along the chain, even at the ends. In the strong stretching limit, the theory recovers the results of Milner et al.[13] and Zhulina et al. [14] Whether corrections for these deviations would contribute to the free energy to the same extent as the entropy for the exchange of ends remains unclear.

Direct comparison of the planar theory to experiments with the surface forces technique is possible. However, the data available due to Kim et al. exposed the surfaces to a bulk solution of micelles,[28] which allows micelles to enter the gap as the separation is increased, thereby changing the reference state and the interaction potential. Dai et al.[24] started with PEO−PS−PEO chains on one of the two surfaces and replaced the solution with pure solvent (toluene in this case) to detect the force during compression−decompression cycles. They observed that attraction arises in the first few cycles but then decreases until the interactions become purely repulsive after many cycles. The separation between planar surfaces at the onset of repulsion also increases with number of cycles. When one surface is bare, ends detach from the other surface to adsorb on it, thus forming bridges that create a strong attraction. As the concentrations on the two surfaces become comparable, the attraction decreases toward that predicted here. However, chains also can leave the surface to form a

population of micelles in solution in equilibrium with the adsorbed chains. Hence, the attraction continues to decrease as interactions with micelles decrease the free energy of the isolated layers. Whether the attraction ultimately disappears or simply falls below the limit of detection is unclear.

By converting our planar case to spherical or cylindrical geometries, we expect to address properties of micellar solutions that are sensitive to interactions, such as the radial distribution function, second virial coefficient, structure factor from light and/or neutron scattering, and the high-frequency modulus.

Acknowledgment. The authors appreciate support from NSF (Division of Engineering Chemical and Transport Systems) through Grants CTS 98-12409 and CTS 01-20421. During the revision process, Christian Ligoure brought to our attention a quite similar effort of his in the 1990s, which was never published.

References and Notes

(1) Pham, Q. T.; Russel, W. B.; Lau, W. *J. Rheol.* **1998**, *42*, 159−76.
(2) Filali, M.; Ouazzani, M. J.; Michel, E.; Aznar, R.; Porte, G.; Appell, J. *J. Phys. Chem. B* **2001**, *105*, 10528−35.
(3) Filali, M.; Aznar, R.; Svenson, M.; Porte, G.; Appell, J. *J. Phys. Chem. B* **1999**, *103*, 7293−7301.
(4) Bhatia, S. R.; Russel, W. B.; Lal, J. *J. Appl. Crystallogr.* **2000**, *33*, 614−17.
(5) Jenkins, R. D. PhD Thesis, Lehigh University, 1991.
(6) Pham, Q. T.; Russel, W. B.; Thibeault, J. C.; Lau, W. *Macromolecules* **1999**, *32*, 5139−5146.
(7) *Hydrophilic Polymers*: *Advances in Chemistry Series 248*; Glass, J. E., Ed.; American Chemical Society: Washington, DC, 1996.
(8) Tam, K. C.; Jenkins, R. D.; Winnik, M. A.; Bassett, D. R. *Macromolecules* **1998**, *31*, 4149−59.
(9) Ma, S. X.; Cooper, S. L. *Macromolecules* **2002**, *35*, 2024−29.
(10) Serero, Y.; Jacobsen, V.; Berret, J.-F.; May, R. *Macromolecules* **2000**, *33*, 1841−7.
(11) Semenov, A. N.; Joanny, J.-F.; Johner, A.; Bonet-Avalos, J. *Macromolecules* **1997**, *30*, 1479−89.
(12) De Gennes, P. G. *J. Phys. (Paris)* **1976**, *37*, 1445−52.
(13) Milner, S. T.; Witten, T. A.; Cates, M. E. *Macromolecules* **1988**, *21*, 2610−19.
(14) Zhulina, E. B.; Borisov, O. V.; Priamistsyn, V. A. *J. Colloid Interface Sci.* **1990**, *137*, 495.
(15) Milner S. T.; Witten, T. A. *Macromolecules* **1992**, *25*, 5495−503.
(16) Johner, A.; Joanny, J.-F. *J. Chem. Phys.* **1992**, *96*, 6257−73.
(17) Bjorling, M. *Macromolecules* **1998**, *31*, 9026−32.
(18) Ball, R. C.; Marko, J. F.; Milner, S. T.; Witten, T. A. *Macromolecules* **1991**, *24*, 693−703.
(19) Li, H.; Witten, T. A. *Macromolecules* **1994**, *27*, 449−57.
(20) Lin, E. K.; Gast, A. P. *Macromolecules* **1996**, *29*, 390−7.
(21) Semenov, A. N.; Joanny, J.-F.; Khokhlov, A. R. *Macromolecules* **1995**, *28*, 1066−75.
(22) Pham, Q. T.; Russel, W. B.; Thibeault, J. C.; Lau, W. *Macromolecules* **1999**, *32*, 2996−3005.
(23) Matsen, M. W. *J. Chem. Phys.* **2002**, *117*, 2351−58.
(24) Dai, L.; Toprakcioglu, C. *Macromolecules* **1992**, *25*, 6000−6.
(25) Bhatia, S. R.; Russel, W. B. *Macromolecules* **2000**, *33*, 5713−20.
(26) Milner, S. T. *J. Chem. Soc., Faraday Trans.* **1990**, *86*, 1349−53.
(27) Netz, R. R.; Shick, M. *Macromolecules* **1998**, *31*, 5105−22.
(28) Kim, H. S.; Lau, W.; Kumacheva, E. *Macromolecules* **2000**, *33*, 4561−67.

MA0349027